Gain Broadening of Two-Stage Tapered Gyrotron Traveling Wave Tube Amplifier

G. S. Park,* J. J. Choi,† S. Y. Park,‡ C. M. Armstrong,§ A. K. Ganguly,* R. H. Kyser,‖ and R. K. Parker
Naval Research Laboratory, Code 6840, Washington, D.C. 20375-5000
(Received 29 August 1994)

The first operation of a two-stage tapered gyrotron traveling wave amplifier employing two tapered waveguide circuits and tapered magnetic fields is reported. Small-signal gain of 30 dB and saturated gain of 25 dB over a 20% bandwidth at an efficiency of 16% have been observed using a 33 kV, 1.5 A electron beam. Comparison with supporting theory is satisfactory.

PACS numbers: 85.10.Jz, 42.52.+x, 52.75.Ms

The continuing need for broadband high-power sources of millimeter-wave radiation has, in recent years, prompted research on fast-wave amplifying mechanisms, such as the gyrotron traveling wave tube (gyro-TWT) interaction [1–3]. This interaction, based on the electron cyclotron maser instability for gyrating electrons in an external magnetic field, has shown itself capable of supporting a saturated gain of 20 dB over a 10% bandwidth with 23% efficiency in a single-stage K_a-band (35 GHz) TE_{11}-mode circuit, using a 90 kV, 1.5 A beam. But, in that experiment [1], it was necessary to suppress incipient oscillations by strongly driving the device. With a two-stage severed circuit, the same researchers [2] achieved 35 dB saturated gain and 16% efficiency over a 7.5% bandwidth. In a C-band (7 GHz) single-stage TE_{11}-mode device, 20 dB saturated gain and 26% efficiency over a 7.25% bandwidth using a 65 kV, 7 A beam was reported [3]. But to avoid spurious oscillations from the absolute instability arising in the presence of multipass reflections, these prior experiments employed relatively high beam voltages and low velocity ratios $\alpha = v_t/v_z$ (i.e., α of the order of unity, or less), where v_t and v_z are the beam electron's transverse and axial velocities.

The prior experiments were not able to achieve gain over a wide bandwidth due to the fundamental nature of the cyclotron maser instability in a nearly uniform system. One means of overcoming the bandwidth limitation is to taper both the axial magnetic field strength and the wave's cutoff frequency along the interaction length, so as to provide a localized region along the device where gyroresonance can be satisfied at all frequencies within the desired band. This novel principle of a distributed wideband amplifier has been previously demonstrated by us in a single-stage K_a-band experiment using a rectangular TE_{10} waveguide with a linearly tapered wide dimension, together with a nonlinearly tapered magnetic field [4]. In that experiment, using a 33 kV, 1.2 A beam with $\alpha = 0.6$, a small-signal gain of 25 dB was achieved over a 30% bandwidth. As this experiment required a round-trip pass for the amplifying radiation at each frequency, window reflections limited the small-signal gain for a "flat" response to about 20 dB. Saturated gain of 17 dB was measured in a narrow band, corresponding to an output power of 5 kW and 9% efficiency. This preliminary experiment demonstrated that the principle of a strongly tapered wideband distributed amplifier was valid, but suffered from the disadvantages of limited saturated gain and stability due to output circuit mismatch and the necessity of operating the experiment in a reflection mode.

In the work reported here, it is shown, for the first time, that two electromagnetically isolated stages of a tapered distributed amplifier can be operated to achieve high small-signal and saturated gain with wide instantaneous bandwidth. This result is significant in its further confirmation of the underlying physical principle of a distributed tapered-parameter gain interaction, and in its realization of gain and bandwidth values of interest for communications and radar applications. With two distinct tapered gain regions separated by a cutoff drift length, as used in the experiment to be reported, the ballistic drift length for electrons between gain regions depends on frequency; this unusual arrangement is not present in other two-stage amplifying interactions, such as the gyroklystron and uniform circuit gyro-TWT.

The experimental setup of the two-stage tapered gyro-TWT is shown in Fig. 1. A 1.5 A, 33 kV annular electron beam, produced from a double anode magnetron injection gun (MIG), is adiabatically compressed to the beam velocity ratio α of 0.7 at the entrance of the tapered waveguide circuit. The two-stage tapered circuit consists of three sections: a linearly down-tapered rectangular waveguide (input section), a 1 in. long waveguide cutoff sever section ($f_{co} = 39.4$ GHz), and a linearly up-tapered rectan-

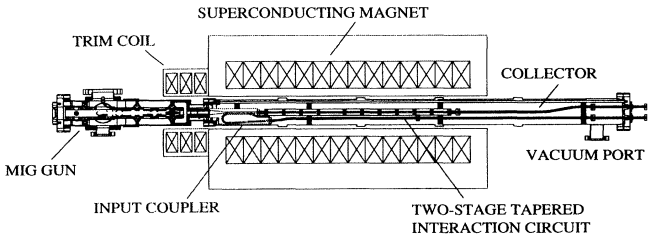

FIG. 1. Layout of two-stage tapered gyro-TWT amplifier.

0031-9007/95/74(12)/2399(4)$06.00 © 1995 The American Physical Society

gular waveguide (output section). The rf drive chain consists of a frequency synthesizer and a 50 W TWT. The rf is injected into the input section through a broadband sidewall directional coupler. The measurements show a coupling value of better than −1 dB and a return loss < -25 dB over the full K_a band (26.5–40 GHz), in good agreement with the 3D electromagnetic code HFSS [5]. The amplified rf signal in the input section is reflected at waveguide cutoff and coupled back to a matched load through the input directional coupler. The amplified rf power in the output section is extracted directly through a 2 in. long linear transition to the K_a-band waveguide. The width of the circuit varies from 0.24 (f_{co} = 24.6 GHz) to 0.15 in. (f_{co} = 39.4 GHz) along an 8 in. length in the input section and from 0.15 to 0.24 in. along a 12 in. length in the output section. The circuit height throughout its axial extent remains constant at 0.14 in. The total length of the two-stage circuit (21 in.) is the same as in the previous single-stage gyro-TWT experiment. The input and output tapering lengths have been designed to provide around 30 dB of total gain. Thin (< 0.001 in.) mica sheets are used as the rf vacuum windows and as dc breaks for monitoring the circuit and collector current. Cold test measurements on the rf windows show a return loss of −23 dB, thereby satisfying the amplifier stability condition regarding reflection instability (round-trip gain less than unity) in both the input and output stages. The magnetic field profile is obtained by using a computer-controlled, 14-coil superconducting magnet system. The individual coil currents required are obtained from a magnetic field synthesis code. To satisfy the beam quality requirement, three water-cooled magnet trim coils are energized in the gun region to insure a flat magnetic field at the cathode. The magnetic field varies from 9.4 at the entrance of circuit to 14.3 kG at the cutoff section in this experiment. The rf power was measured using a peak power analyzer calibrated by a dry calorimeter.

Figure 2 shows the saturation of the two-stage tapered gyro-TWT using a 50 W TWT driving amplifier. The TWT generates about 50 W from 32 to 37 GHz. Electronic efficiency of 16% has been measure33 kV and 1.5 A with an operating frequency of 36 GHz. A maximum power level of 10 kW was measured at 33 kV and 1.9 A with little degradation of bandwidth and efficiency. By decreasing the gain per stage in the two-stage circuit, the linear gain has improved from 23 to 30 dB and saturated gain increased from 17 to 25 dB. In the first stage the input signal was amplified to 9 dB and produced the velocity modulation of the electron beam. As expected, the reduced gain per stage of the two-stage configuration is found to significantly improve the gain flatness across the band over a single-stage high-gain design. The gain fluctuation of ±5 dB at the linear gain of 23 dB observed previously with the single-stage tapered gyro-TWT is observed to decrease significantly to about ±2 dB at 30 dB gain for the two-stage tapered gyro-TWT. The gain fluctuation is a sensitive function of the reflection coefficients of the circuit and the gain of the amplifier. In general, the larger the per-stage gain of the device, the larger the fluctuation amplitude in the output signal. The guide magnetic field profile used in the experiments is shown in Fig. 3.

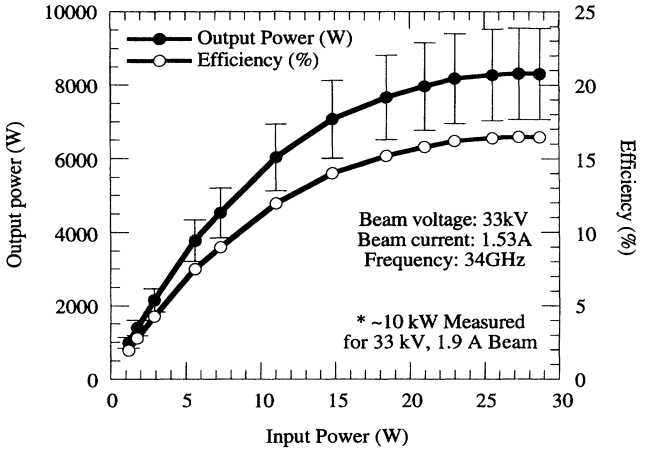

FIG. 2. Drive curve.

The measured performance characteristics of the two-stage tapered gyro-TWT is compared with numerical simulations using the self-consistent slow-time-scale nonlinear code [6] developed for such a device. The nonlinear theory is based on a slow-time-scale formulation of the beam-wave interaction in a two-stage tapered interaction circuit of rectangular cross section. In this formulation, the electromagnetic field is expanded as a superposition of unperturbed TE and TM modes of an empty waveguide. Maxwell's equations are averaged over a wave period and the slow-time-scale equations are derived for the evolution of the amplitude and phase of each mode as driven by

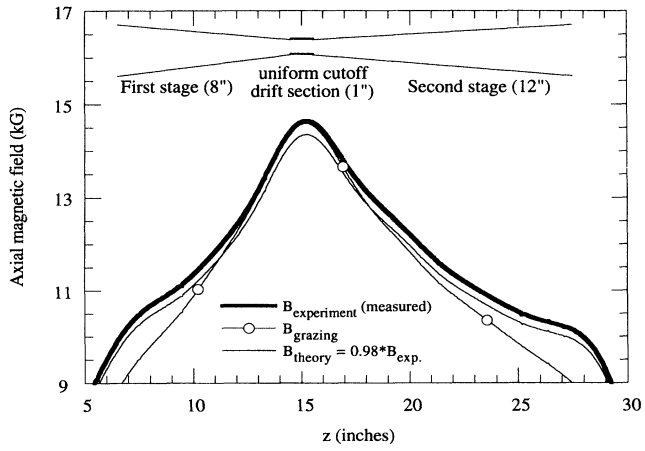

FIG. 3. Guide magnetic field profile.

an electron beam in the presence of a guide magnetic field. The time-averaged field equations are integrated simultaneously with three-dimensional Lorentz force equations that determine the particle orbits. The theory includes the effects of the guiding center motion, axial velocity spread, and nonuniform guide magnetic field. Electrostatic space charge forces are neglected. We also ignore the interaction between the forward propagating electron beam and the reflected eletromagnetic field in the input section of the two-stage amplifier. It is assumed that the radiation fields are cut off in the drift region.

The gain and bandwidth of the device are calculated for a 33 kV, 1.5 A beam with $\alpha = 0.7$ at the entrance to the first stage. The simulations of the beam optics by Hermannsfeldt code show an $\alpha \sim 0.7$ and an axial velocity spread $\sim 4\%$. The input signal power is 15 W. We first show calculated results for a guide magnetic field nonlinearly tapered to maintain "grazing" condition at all axial positions. The gain is plotted in Fig. 4 as a function of frequency for different axial velocity spreads of the electron beam. For this guide magnetic field profile, calculations indicate an efficiency of 27% (13.3 kW output power) and a 30% bandwidth for a cold beam. The instantaneous bandwidth of the two-stage tapered gyro-TWT with a fixed magnetic field profile and initial velocity ratio is extremely sensitive to the spread in the axial velocity of the electrons. This is evident in Fig. 4 where the gain versus frequency curves for $\delta v_z/v_z > 0$ have sharp dips at certain frequencies and the 3 dB bandwidth at $\delta v_z/v_z = 4\%$ is reduced to 10%. The net gain (at the exit of the second stage) within the 3 dB band, however, decreases very slowly with increase in the velocity spread. The peak gain at each frequency is also insensitive to the beam thermal effects. This is due to the fact that the gain at each frequency peaks at an axial position near its cutoff region where resonant beam-wave interaction occurs with negligible Doppler shift, i.e., $\omega = \omega_c(z = z_{cr}) \approx s\Omega$. Here, ω_c is the cutoff frequency at $z = z_{cr}$, s is the cyclotron harmonic number, and Ω is the relativistic cyclotron frequency ($\Omega = \Omega_0/\gamma = eB/\gamma m_0$). A closer examination of the phase space distribution of the electrons reveals that the dips in the gain curves in the present case at nonzero velocity spreads correspond to frequencies where the bunching is poor at the end of the drift region. It should be pointed out that the drop in net gain at the exit of the device is not always caused by poor bunching. In some cases the electron beam was properly bunched in the first stage and in the drift region. As the bunched beam enters the second stage, it is quickly trapped in the potential bucket yielding high efficiency and gain at an axial position near the resonant region. But a detrapping of the beam can occur if the magnetic field profile and the axial wave vector profile are not correctly maintained and the gain at the exit is lowered from its peak value. A detailed discussion of these effects will be given in a separate publication.

The frequencies of sharp drop in gain depend on the magnetic field profile, beam voltage and current, the velocity ratio, the axial velocity spread, and the circuit parameters. These frequencies can be shifted by adjusting the magnetic field profile when all other parameters are fixed. The grazing magnetic field profile provides optimum bandwidth at zero velocity spread for the parameters in Fig. 4. A different guide magnetic field profile is necessary to optimize the bandwidth for a warm beam. The experiment showed a small bandwidth at grazing magnetic field, in agreement with results in Fig. 4, for $\delta v_z/v_z = 4\%$. The theory and experiment are compared in Fig. 5, where the saturated gain is plotted as a function of frequency for a beam with $\delta v_z/v_z = 4\%$. The calculated results for zero velocity spread are also

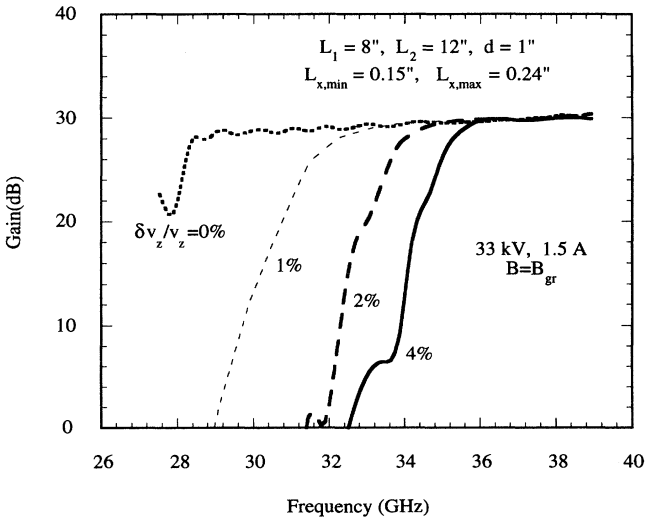

FIG. 4. Plot of gain vs frequency in a grazing magnetic field.

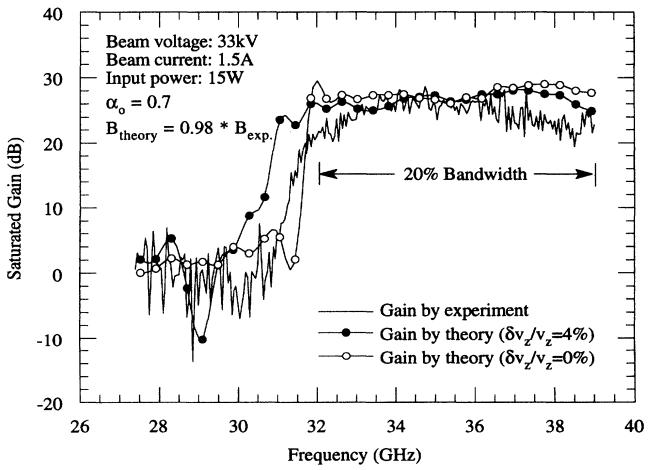

FIG. 5. Measured gain and input and output power vs frequency, and comparison with theory.

shown for reference. The theory agrees very well with the experiment both qualitatively and quantitatively, if the calculations are done with a guide magnetic field 2% lower than the experimental magnetic field, i.e., $B_{\text{theo}}(z) = 0.98B_{\text{expt}}(z)$, as shown in Fig. 3. The small discrepancy between the theoretical and experimental magnetic field profile may be due to the uncertainties in the magnetic field alignment, the velocity ratio, and the velocity spread. From Figs. 4 and 5, it is seen that the bandwidth at $\delta v_z/v_z = 4\%$ is increased to 20% in the experimental magnetic field profile compared to 10% bandwidth in the grazing magnetic field. On the other hand, the bandwidth at $\delta v_z/v_z = 0$ is lowered from 30% in the grazing magnetic field to 20% in the experimental magnetic field. The tapered guide magnetic field for maximum bandwidth will deviate from the grazing condition for the realistic electron beam.

Since the gain per stage is reduced (14 rather than 25 dB) in the two-stage device, stable amplifier operation is possible at higher electron beam α than for the single-stage device, and higher device efficiency can be expected. The reflective instability that limits the performance of the single-stage tapered gyro-TWT is now not expected to be a dominant issue. The first two-stage gyro-TWT experiment proves the feasibility of a stable, broadband amplifier with a total gain of $\sim$ 30 dB, an electronic efficiency of (20–30)%, and an instantaneous bandwidth >20% for α's between 0.6 and 0.8 and $\delta v_z/v_z = 4\%$. Key issues to be confronted in optimizing the efficiency and bandwidth of the two-stage tapered gyro-TWT are electron beam quality and accurate magnetic field profiling.

The authors would like to acknowledge useful discussions with Professor J. L. Hirshfield and Professor V. L. Granatstein. Also the technical support of B-K Systems is acknowledged. This work is supported by the Office of Naval Research.

*Present address: Omega-P, Inc., New Haven, CT 06520.
†Present address: Science Application International Corporation, McLean, VA 22102.
‡Present address: Department of Physics, Pohang Institute of Science and Technology, Pohang, Korea, and Omega-P Inc.
§Present address: Northrop Corporation, Rolling Meadows, IL 60008.
‖Present address: B-K Systems, Inc., Rockville, MD 20850.

[1] L. R. Barnett *et al.*, Phys. Rev. Lett. **63**, 1062 (1989).
[2] K. R. Chu *et al.*, in *IEDM Technical Digest* (Institute of Electrical and Electronic Engineers, New York, 1990), pp. 699–702.
[3] R. S. Symons *et al.*, IEEE Trans. Microwave Theory Tech. **MTT-29**, 794 (1981).
[4] G. S. Park *et al.*, in *IEDM Technical Digest* (Institute of Electrical and Electronic Engineers, New York, 1991), pp. 779–781; IEEE Trans. Plasma Sci. **PS-22**, 536 (1994).
[5] HP High Frequency Structure Simulator, Version A.02.01, Hewlett Packard Co. and Ansoft Co.
[6] A. K. Ganguly *et al.*, Int. J. Electron. **53**, 641–658 (1982); IEEE Trans. **ED-31**, 474–804 (1984).